

Oxidation state of vanadium in amorphous MnV_2O_6 formed during discharge–charge cycle and the improvement of its synthesis condition

Takahiro Morishita ^a, Hidetaka Konno ^b, Yasuo Izumi ^c, Michio Inagaki ^{a,*}

^a Faculty of Engineering, Aichi Institute of Technology, Yakusa, Toyota 470-0392, Japan

^b Laboratory Advanced Materials Chemistry, Graduate School of Engineering, Hokkaido University, Sapporo 060-8628, Japan

^c Tokyo Institute of Technology, Interdisciplinary Graduate School of Science and Engineering, Nagatsuta 4529, Midori-ku, Yokohama 226-8502, Japan

Received 17 March 2006; received in revised form 15 May 2006; accepted 27 May 2006

Abstract

Crystalline powders of anhydrous MnV_2O_6 were successfully synthesized at a temperature below 200 °C under autogenous hydrothermal condition. MnV_2O_6 powders, which were synthesized using high concentration solutions, more than 0.1 mol/L, gave a relatively high reversible capacity of 600 mA h/g and interesting cyclic performance, reversible capacity increasing to more than an initial charge capacity after the 3rd or 4th cycle of charge–discharge. The change in oxidation state of V ion on the course of the 1st discharge–charge process was investigated by different techniques, such as XAFS and XPS. During discharging, V^{5+} was found to change gradually to V^{4+} , but it returned back completely to V^{5+} on charging process. The thinner particles of MnV_2O_6 crystals with rod-like morphology were synthesized at 135 °C, and much better anodic performance was achieved, much smaller irreversible capacity as about 300 mA h/g, stable reversible capacity as 600 mA h/g, and 100% Coulombic efficiency.

© 2006 Published by Elsevier B.V.

Keywords: Lithium ion secondary batteries; Manganese vanadate; Anode; Hydrothermal synthesis

1. Introduction

Lithium ion rechargeable batteries have high current and power densities in comparison with other rechargeable batteries, such as lead, nickel cadmium and nickel hydrogen batteries [1]. Commercial cells of lithium ion rechargeable batteries have developed by selecting suitable electrode materials in both cathode and anode, such as LiCoO_2 and graphite, respectively [2]. However, there are still strong demands to have better performance of batteries, high power and high rate charge–discharge process [3].

Manganese vanadate MnV_2O_6 with brannerite structure was proposed to be used for the anode of lithium ion rechargeable batteries [4] and then studied on its preparation, structure and anodic performance by different groups [5–10]. Anhydrous crystalline powders of MnV_2O_6 were synthesized through solid state reaction between Mn_2O_3 and V_2O_5 [5], but nonstoichiometric

composition of manganese vanadate was required in order to have anodic activity [4]. The synthesis of hydrous manganese vanadate powders were performed by coprecipitation from aqueous solutions of $\text{Mn}(\text{NO}_3)_2$ and NaVO_3 [6,7]. In order to have anodic activity in lithium ion rechargeable batteries, anhydrous manganese vanadate had to be obtained by the heat treatment of these hydrous manganese vanadate powders, but a relatively low anodic activity, low capacity and low Coulombic efficiency, was obtained [4]. In order to improve anodic activity of these powders, their ozonation was proposed [6]. The preparation of anhydrous manganese vanadate was also reported through the heat treatment of aqueous gels containing manganese and vanadium ions with a polymer at 400 °C [8].

In our previous papers [9,10], anhydrous manganese vanadate powders were successfully synthesized under autogenous hydrothermal condition and also through coprecipitation process under normal pressure. Some of manganese vanadate powders synthesized were found to have relatively high capacity as 600–700 mA h/g and an interesting charge–

* Corresponding author.

E-mail address: ina@aitech.ac.jp (M. Inagaki).

discharge performance, reversible capacity increasing to more than the initial charge capacity after the 3rd or 4th cycle. These powders were synthesized from a high concentration solution of manganese acetate, higher than 0.1 mol/L, with the dispersion of vanadium pentoxide and characterized by strong 110 diffraction peak, relative to other peaks, and by thin rode-like morphology. In order to understand and to improve the anode performance of these powders, it was strongly desired to know the changes in oxidation state of cations, Mn and V, during charge–discharge process. However, the starting crystalline manganese vanadate was found to change to amorphous one even after the first cycle of charge–discharge, which made us to understand the changes in oxidation state of cations difficult.

In the present work, therefore, XPS and XAFS measurements were performed on the powders sampled on the course of discharge and charge processes in a test cell of lithium ion rechargeable batteries and oxidation states of manganese and vanadium ions were discussed. These experimental results were fed back to the synthesis under hydrothermal condition and the manganese vanadate powders with better performance were successfully obtained.

2. Experimental

2.1. Synthesis of manganese vanadate powders

The starting materials used were reagent grade manganese acetate [$\text{Mn}(\text{CH}_3\text{COO})_2 \cdot 4\text{H}_2\text{O}$, 99.0% purity, Nakalai Tesque Ltd.] and vanadium pentoxide [V_2O_5 , 99.99% purity, High Purity Chemicals Ltd.]. Preparation of manganese vanadate powder was carried out by following procedures; aqueous solutions of $\text{Mn}(\text{CH}_3\text{COO})_2$ and V_2O_5 were mixed to be the V/Mn molar ratio of 2 and metal ion concentration was controlled to be 0.1 mol/L, where undissolved V_2O_5 particles were suspended and the pH value was kept at about 4.0. The mixed solution of 18 mL was taken into a 25-mL container of Teflon-lined stainless steel. After sealing the container, it was heated either at 200 °C for 5 h or at 135 °C for 1 h with constant rotation of 10 rpm. After this treatment, the precipitates formed were recovered by washing, centrifuging and drying. The detailed procedure for the synthesis of manganese vanadate was reported in our previous paper [9].

The crystal structure of the precipitates thus obtained was examined by X-ray powder diffraction (XRD: Rigaku RINT-2500) with $\text{CuK}\alpha$ radiation. Morphology of the powder was observed from transmission electron microscope (TEM: JEOL JEM-2010) with acceleration voltage of 200 kV.

2.2. Anodic performance for lithium ion rechargeable batteries

The electrode to determine anodic performance was prepared by mixing the sample manganese vanadate powder with acetylene black as an electric conductor and polyvinylidene difluoride (PVDF) as a binder in a mass ratio of 70:20:10, and pasting on a thin film of Ni. Li metal was used as counter-electrode. The electrolyte solution was the mixture of ethylene carbonate (EC) and diethyl carbonate (DEC) in equal volume

ratio, in which 1 mol/L LiClO_4 was dissolved. The anodic performance was determined in the range of potential at 0.0–2.5 V with a current density of 50 mA/g at room temperature in a glove box filled with Ar gas. Discharge and charge cycles were usually performed up to 10th, except up to 50th to check if cyclic performance for the sample renewed its synthesis conditions. The details on the preparation of anode and the test cell used were reported in our previous paper [10].

2.3. X-ray absorption fine structure analysis and X-ray photoelectron spectroscopy

In order to understand the changes in oxidation state of vanadium and manganese ions during lithium ion insertion (discharge) and de-insertion (charge) into the manganese vanadate electrode, the anode materials were sampled out at different stages in the 1st cycle of discharge–charge process with a constant current density of 50 mA/g. X-ray absorption fine structure analysis (XAFS: synchrotron radiation facilities of Photon Factory in High Energy Accelerator Research Organization, Tsukuba) and X-ray photoelectron spectroscopy (XPS: VG ESCALAB MkII) were used for this purpose.

When the potential of the cell reached down to either 0.7 or 0.0 V during discharge process and up to 0.7 and 2.5 V during charge process, the current being supplied was cut down and then the anode was picked out from the cell in a glove box of Ar atmosphere. The anode material thus obtained was packed into a plastic bag with the electrolyte solution under vacuum. For XAFS measurement, the sample either packed into a plastic bag or picked out just before measurement was used. Just before XPS measurement, the samples were separated from electrolyte solution by evacuating at room temperature for 12 h.

From XAFS measurement, vanadium K-edge absorption spectra were measured at 290 K in transmission mode at the beam line 12C of the storage ring operated at 2.5 GeV and the current of 290–400 mA. XPS measurements were carried out at lower than -150 °C to avoid possible changes of oxidation state by X-ray irradiation (Mg $\text{K}\alpha$, 14 kV, 20 mA) in vacuum. Although the spectrometer was calibrated correctly using Au 4f peaks, the binding energy (E_B) values obtained in the present work were not very accurate due to large charge-up shifts: binding energy correction was carried out by using C 1s peak for PVDF and O 1s peak for oxide ion. Accordingly, the chemical states were mainly evaluated by the differences in E_B between major peaks and the spectrum profiles including position and splitting of satellite peaks. X-ray satellites were subtracted and peak separation was done only for s orbital peaks by using Gaussian/Lorentzian product functions as described previously [11].

3. Results and discussion

3.1. Manganese vanadate synthesized

For the sample manganese vanadate powder synthesized at 200 °C under hydrothermal condition, XRD pattern, morphology under TEM and cyclic performance for discharge–charge in

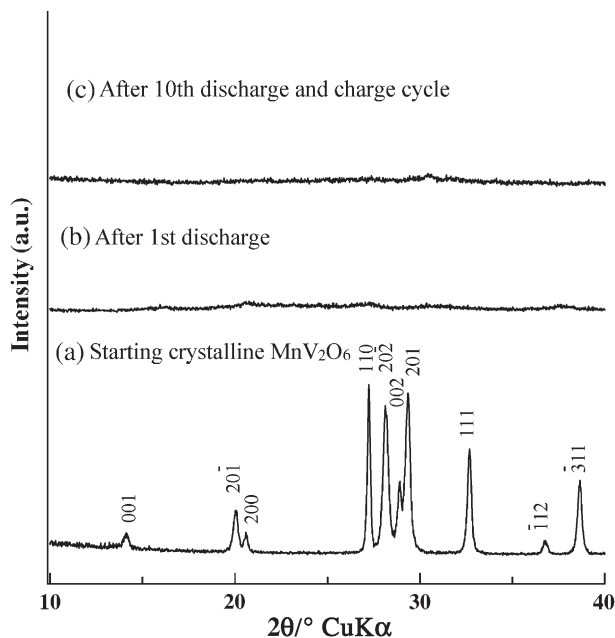


Fig. 1. X-ray powder diffraction patterns of manganese vanadate synthesized at 200 °C.

lithium ion rechargeable batteries are shown in Figs. 1a–c, respectively. The powder obtained was crystalline, a single phase of brannerite structure. Strong 110 diffraction peak (Fig. 1a) and rod-like morphology (Fig. 2a) are characteristics of interesting cyclic performance, a sudden increase in capacity after the 4th cycle, as shown in Fig. 3. The same cycling performance was observed and discussed in our previous papers [9,10], strongly depending on the synthesis conditions and being characterized by strong 110 diffraction peak in XRD pattern.

3.2. Oxidation state of vanadium ions

On this manganese vanadate powder synthesized at 200 °C, its crystalline structure and rod-like morphology were lost and

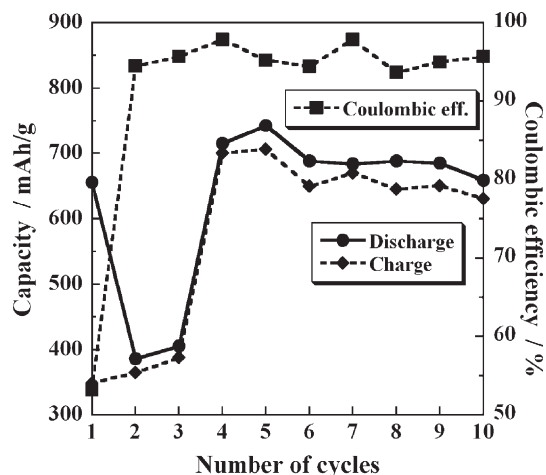


Fig. 3. Cyclic performance of manganese vanadate synthesized at 200 °C.

became amorphous, even after the 1st cycle of discharge–charge, as reported previously [9,10]. XRD patterns of the powders after the 1st discharge–charge cycle and also the 10th cycle are shown in Fig. 1b and c, respectively. The diffraction peaks for brannerite structure were broadened and weakened. It was difficult to identify the peaks, even after the 1st cycle and they disappeared completely after the 10th cycle. The peaks due to Ni film and probably due to PVDF binder used were often observed because these XRD patterns were measured on the films used as electrode during insertion (discharge) and deinsertion (charge) in the electrolyte. In the TEM photograph, the particles with irregular shapes were observed, as shown in Fig. 2b, which were supposed to be in amorphous state because of no diffraction spots in electron diffraction pattern shown as an inserted figure in Fig. 2b.

On four powders which were discharged down to 0.7 and 0.0 V and also re-charged up to 0.7 and 2.5 V on the course of the 1st discharge–charge cycle, the spectra of XAFS and XPS were measured using the films containing carbon black and binder PVDF, and compared with those observed on as-synthesized powder, without any electrochemical treatment.

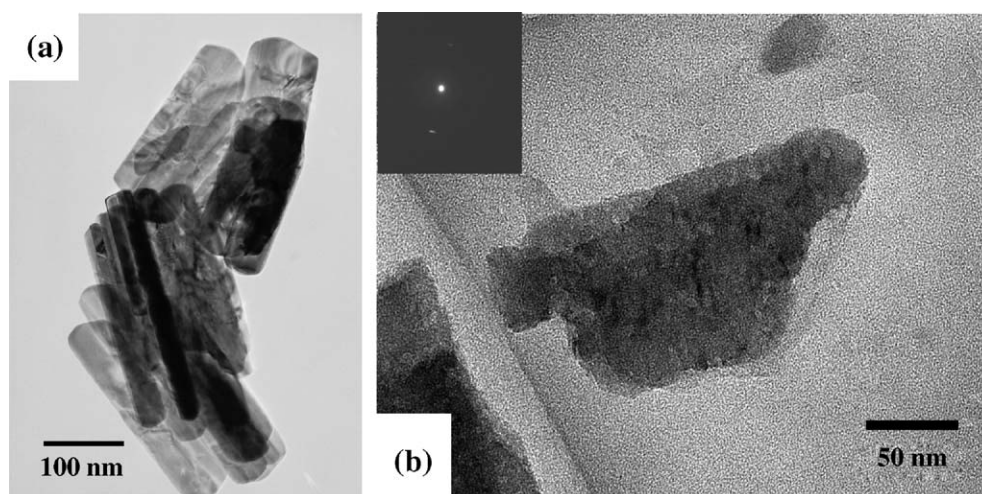


Fig. 2. Transmission electron microscope images of manganese vanadate synthesized at 200 °C: (a) as-prepared crystalline powders and (b) after 1st discharge process.

V k-edge XAFS spectra at around absorption edge of vanadium were shown in Fig. 4a for the sample powders on the way of discharging, together with those for the references, *i.e.*, V_2O_4 and V_2O_5 in which the oxidation state of the vanadium ions was 4+ and 5+, respectively, and in Fig. 4b for the sample powders on the way to charging. From the comparison of the shapes of absorption edge in XAFS spectra, especially based on the absorption edge energy, the starting manganese vanadate was found to contain V^{5+} . On the other hand, the powders on the way of discharging (discharged down to 0.7 and 0.0 V) were reasonably supposed to contain V^{4+} . The content of reduced ion V^{4+} seemed to be higher in the latter case than in the former (Fig. 4a). On re-charging, the spectra became similar to that for V_2O_5 relatively quickly with increasing voltage to 0.7 and then 2.5 V (Fig. 4b). The powders on re-charging up to 0.7 V seems to contain a little higher concentration of V^{5+} than those on discharging down to 0.7 V, as shown in Fig. 4b.

The XPS spectra of Mn and V are shown for the specimens as-prepared, discharged down to 0.7 and 0.0 V, and charged up

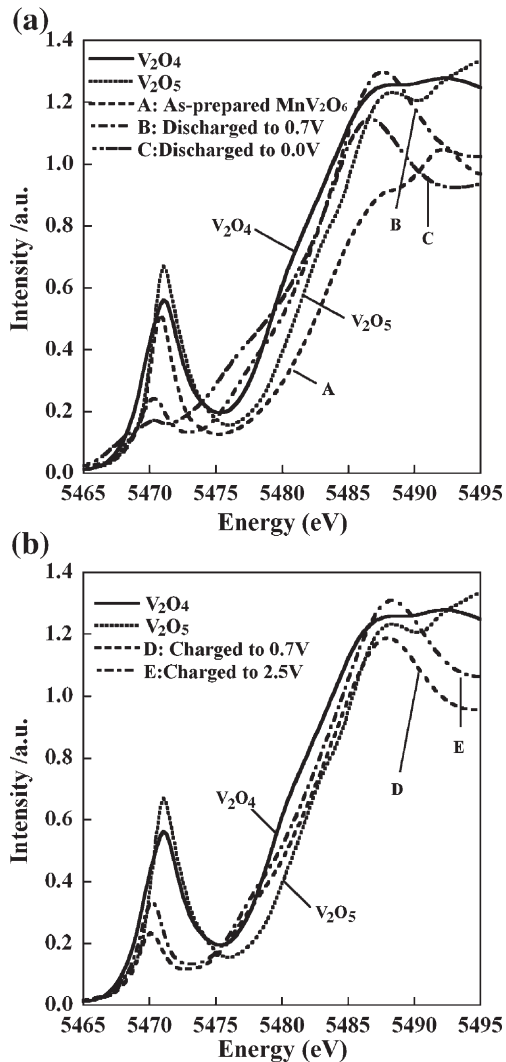


Fig. 4. V K-edge XAFS spectra of manganese vanadate powders: (a) the powders as-synthesized and discharged down to 0.7 and 0.0 V, with the references V_2O_4 and V_2O_5 ; and (b) the powders charged up to 0.7 and 2.5 V.

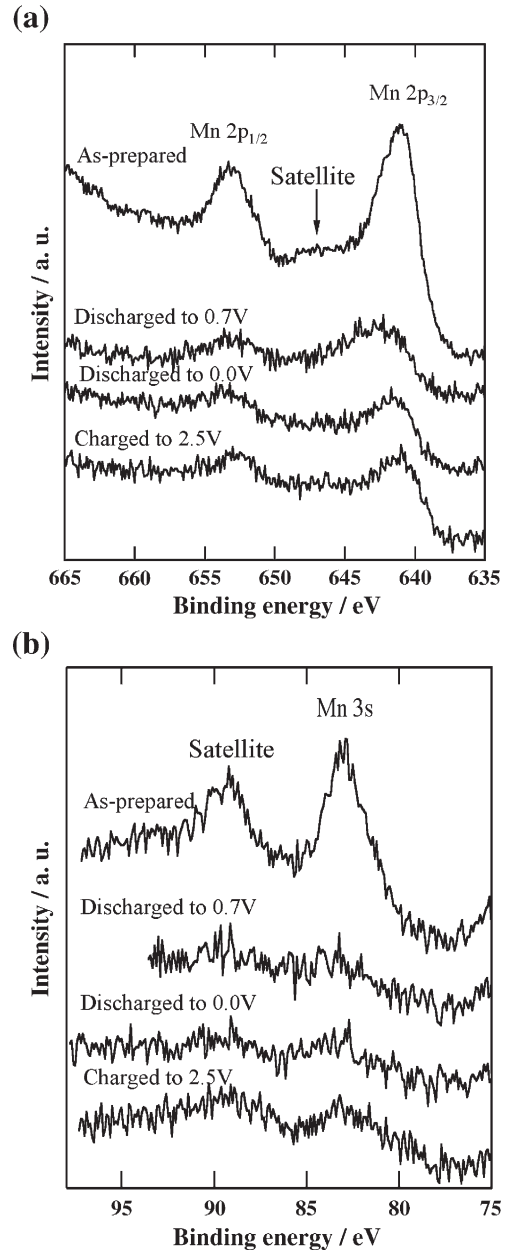


Fig. 5. XPS spectra of Mn 2p (a) and 3s (b) for the specimens as-prepared and discharge down to 0.7 and 0.0 V, and charged up to 2.5 V.

to 2.5 V in Figs. 5 and 6, respectively. It is evident from the profile of spectrum and the position of satellite peak for the as-prepared specimen that manganese ions in the specimen at open circuit potential are divalent [12]. This is well supported by the satellite splitting of Mn 3s peak for this specimen, 6.2 eV, as shown in Fig. 5b, since manganese species of lower valence give a splitting smaller than 5.5 eV [12,13]. The binding energy (E_B) difference between Mn $2p_{3/2}$ and V $2p_{3/2}$ ($\Delta E_B[\text{Mn}-\text{V}]$) was 123.9 eV for this specimen. These features on the spectra of Mn and V ions are distinguished for the specimens at discharged down to 0.0 V and charged up to 2.5 V in Figs. 5a and 6a, although they are ambiguous for the discharged specimen at 0.7 V. It should be noted here that it is unreasonable to evaluate the splitting smaller than 6 eV in Fig. 5a irrespective

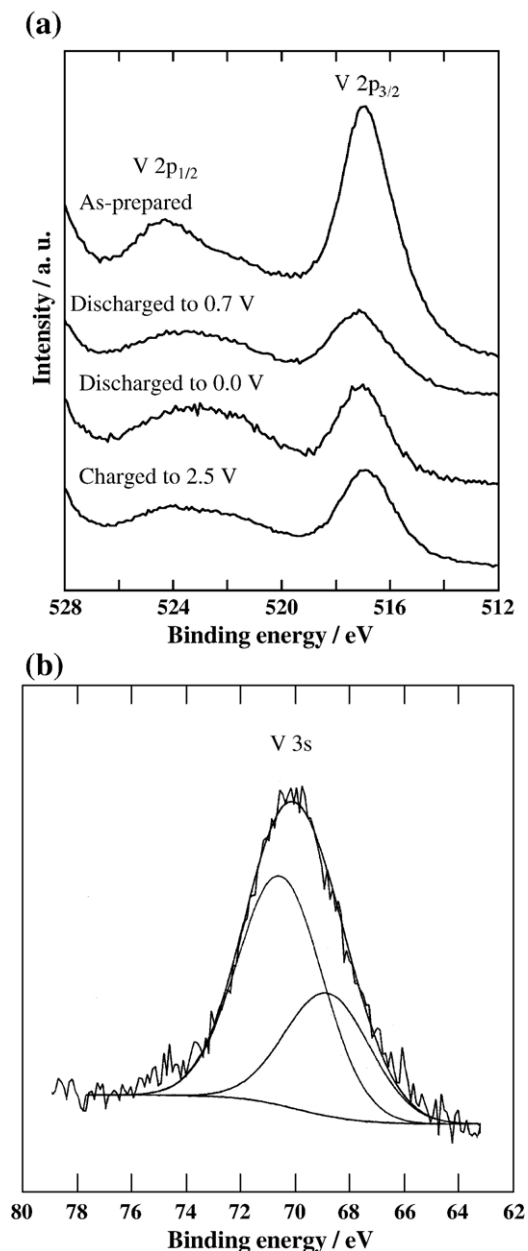


Fig. 6. XPS spectra of V 2p for the specimens as-prepared and discharge down to 0.7 and 0.0 V, and charged up to 2.5 V (a) and that of V 3s for the specimen discharged down to 0.7 V (b).

of noisy spectra. The $\Delta E_B[\text{Mn}-\text{V}]$ values for 0.7 and 0.0 V specimens were 125.4 eV and 124.6 eV, and for the 2.5 V specimen it decreased again to 124.1 eV, which is almost the same with the value for as-prepared (123.9 eV). This change is understandable by considering that only the valence of vanadium ion decreases with Li^+ ion insertion, since it has been reported that $E_B[\text{V } 2p_{3/2}]$ for V_2O_4 is about 1 eV lower than that of V_2O_5 [14].

The formation of V(IV) state is verified by V 3s spectrum shown in Fig. 6b for the discharged specimen down to 0.7 V. The spectrum is broad (FWHM=4.2 eV) for single component V 3s spectrum, and can be separated into two components (FWHM=3.65 eV) at 69.0 eV and 70.8 eV. These E_B values

may have some errors due to the charge-up correction and the calculation for peak separation, but reasonably agree with those of V(IV) and V(V) states [14]. Incidentally, FWHM of V 3s spectrum was 3.86 eV for the as prepared specimen and 3.80 eV for the specimen charged up to 2.5 V. The results by XPS were consistent with those by XAFS (Fig. 4) described above.

From XAFS and XPS analyses, the oxidation state of vanadium ions in manganese vanadate was supposed to change from 5+ in as-synthesized powder to 4+ in the powder discharged down to 0.0 V, and by charging it returned from 4+ to 5+. It had to be pointed out that the reduction of vanadium ion from 5+ to 4+ seemed not to be completed by the first discharge process, but its oxidation state with 4+, which was formed by the previous reduction process, seemed to be re-oxidized to 5+ completely.

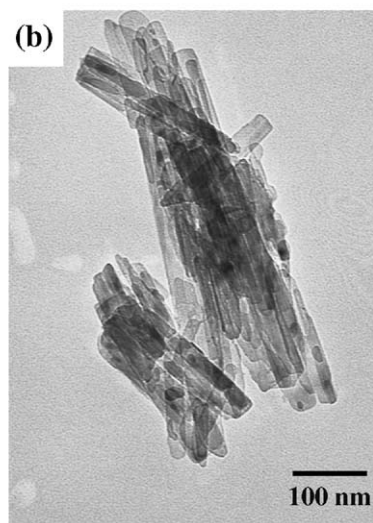
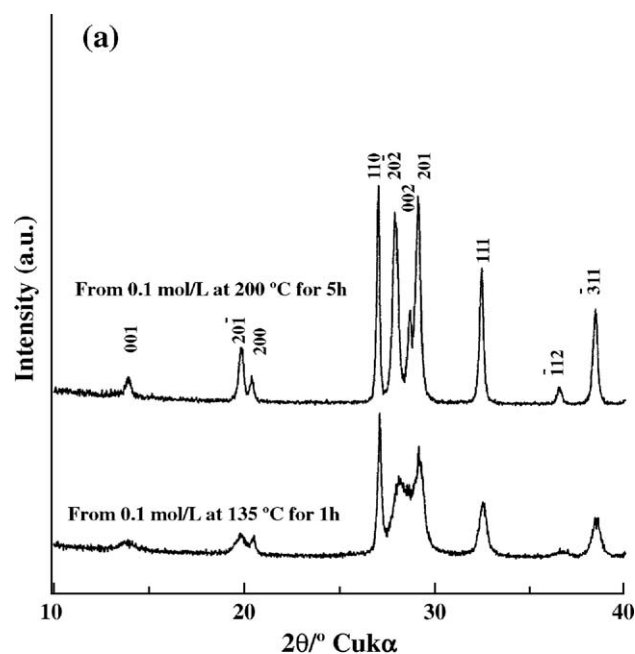


Fig. 7. Manganese vanadate powder synthesized at 135 °C: (a) XRD pattern and (b) TEM image.

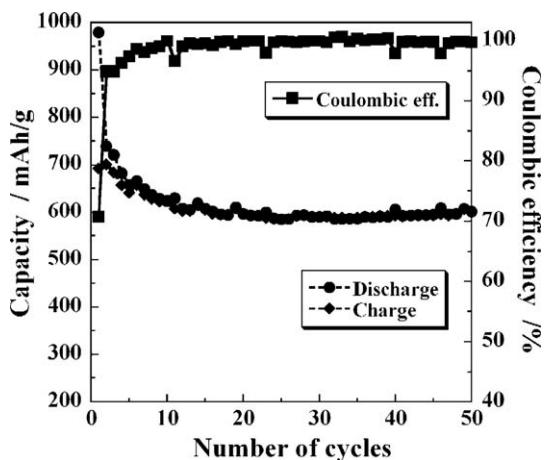


Fig. 8. Cyclic performance of manganese vanadate powder synthesized at 135 °C.

3.3. Renewal of the synthesis of manganese vanadate powder and its anodic performance

Most of the electrochemical reactions occurred at the interfaces between the electrode material and the electrolyte, and proceeded into the inside of the electrode material. In the present work, lithium insertion into manganese vanadate is reasonably supposed to proceed slowly from the surface of its crystals, which may be suggested by the results of XPS analysis that the change in oxidation state of vanadium ions seemed not to be completed even after discharging down to 0.0 V in the first cycle, though XPS gave the information on the surface of the crystals. In other words, the crystals of the present manganese vanadate may be too large to complete the reduction of vanadium ions in the crystals during the first discharge process. This supposition seems to agree with the experimental facts that manganese vanadate electrode shows very high irreversible capacity and that the powder synthesized at 200 °C in the present work needs few discharge–charge cycles to reach stability. To improve this cyclic performance in manganese vanadate electrode, much thinner crystals were tried to be synthesized.

The powder of crystalline manganese vanadate was synthesized once again under hydrothermal condition, at a lower temperature for a shorter time than the case described before (Section 3.1), *i.e.*, at 135 °C for 1 h, other conditions being kept the same as before. XRD pattern and TEM image of the powder thus synthesized are shown in Fig. 7a and b, respectively. XRD pattern of the powder (Fig. 7a) shows a strong 110 diffraction peak, as before (Fig. 1a) and particle morphology is rod-like, but much thinner than before (compared to Fig. 2a).

On the film formed from the powder newly synthesized, discharge–charge cycles were performed up to 50 cycles under exactly the same procedure as before. Cyclic performance obtained is shown in Fig. 8. Discharge capacity at the 1st cycle is not so high, but charge capacity is relatively high (about 70% of discharge capacity), in other words, irreversible capacity is relatively small, as about 300 mA h/g, and Coulombic efficiency

is relatively high, almost 100%, in comparison with the previous powder (Fig. 3). Also it has to be pointed out that discharge and charge capacities decrease slightly and quickly saturate by cycling. The capacity leveled off is 600 mA h/g.

The results on newly synthesized powder proved that thinner crystal of manganese vanadate is desirable. In order to get high anodic performance of manganese vanadate; therefore, low temperature synthesis under hydrothermal condition is necessary.

4. Conclusions

Manganese vanadate crystals, which were synthesized under autogenous hydrothermal condition at 200 °C for 5 h and had rod-like morphology, were changed to amorphous state by the 1st cycle of discharge (insertion of lithium) and charge (de-insertion of lithium) in lithium ion rechargeable batteries. From XAFS and XPS measurements on the samples discharged and charged to different stages in the 1st cycle, vanadium ions were confirmed to change partly from V^{5+} in the as-synthesized MnV_2O_6 to V^{4+} after being discharged down to 0.0 V and to return quickly to V^{5+} during charging. Based on the experimental results on the change in oxidation state of V ions, thinner rod-like particles of MnV_2O_6 were synthesized under much mild conditions than before, *i.e.*, at 135 °C for 1 h, and they gave much better anodic performance, much smaller irreversible capacity as 300 mA h/g, stable reversible capacity as 600 mA h/g and 100% Coulombic efficiency.

On manganese vanadate, in the present work, a high reversible capacity with a relatively small irreversible capacity was obtained by changing the synthesis condition. However, many problems are still remained to be solved; where lithium ions are inserting in amorphous manganese vanadate, why the capacity can go to 600–700 mA/g, why crystalline manganese vanadate changes to amorphous state during the first discharge process, etc.

Acknowledgement

The present work was partly supported by a grant of the Frontier Research Project “Materials for the 21st Century – Materials Development for Environment, Energy and Information” from the Ministry of Education, Culture, Sports, Science and Technology. The XAFS experiments were performed under the approval of the Photon Factory Proposal Committee (2002G 284).

References

- [1] T. Ohzuku, A. Ueda, M. Nagayama, Y. Iwakoshi, H. Komori, *Electrochim. Acta* 38 (1993) 1159.
- [2] K. Sawai, A. Ueda, M. Nagayama, Y. Iwakoshi, H. Komori, *Denki Kagaku* 61 (1993) 715.
- [3] K. Miyayama, S. Suzuki, *Mater. Stage 3* (2003) 37.
- [4] Y. Piffard, F. Leroux, D. Guyomard, J.-L. Mansot, M. Tournoux, *J. Power Sources* 68 (1997) 698.
- [5] V.L. Zolotavin, V.N. Bulygina, I.Y. Bezukov, *Russ. J. Inorg. Chem.* 15 (1970) 222.

- [6] F. Leroux, Y. Piffard, G. Ourvard, J.L. Mansot, D. Guyomard, Chem. Mater. 11 (1999) 2948.
- [7] J.H. Liao, T. Drezen, F. Leroux, D. Guyomard, Y. Piffard, Eur. J. Solid State Inorg. Chem. 33 (1996) 411.
- [8] S.S. Kim, H. Ikuta, M. Wakihara, Solid State Ionics 139 (2001) 57.
- [9] M. Inagaki, T. Morishita, M. Hirano, V. Gupta, Solid State Ionics 156 (3–4) (2003) 275.
- [10] T. Morishita, K. Nomura, T. Inamasu, M. Inagaki, Solid State Ionics 176 (2005) 2235.
- [11] H. Konno, T. Nakahashi, M. Inagaki, Carbon 35 (1997) 669.
- [12] J.S. Foord, R.B. Jackman, G.C. Allen, Philos. Mag., A 49 (1984) 657.
- [13] V. Di Castro, G. Polzonetti, J. Electron Spectrosc. Relat. Phenom. 48 (1989) 117.
- [14] C.N.R. Rao, D.D. Sarma, S. Vasdevan, M.S. Hedge, Proc. R. Soc. Lond., A 367 (1979) 239.